Forecasting Turbine Icing Events

Davis, Neil; Hahmann, Andrea N.; Clausen, Niels-Erik; Zagar, Mark

Published in:
Proceedings of EWEA 2012 - European Wind Energy Conference & Exhibition

Publication date:
2012

Document Version
Publisher's PDF, also known as Version of record

Forecasting Turbine Icing Events

Neil Davis*[1,2], Andrea Hahmann[1], Niels-Erik Clausen[1], and Mark Zagar[2]

[1] *DTU Wind Energy; Roskilde, Denmark*
[2] *Vestas Technology R&D; Aarhus, Denmark*

April 16, 2012

Summary

In this study, we present a method for forecasting icing events. The method is validated at two European wind farms in with known icing events. The icing model used was developed using current ice accretion methods, and newly developed ablation algorithms. The model is driven by inputs from the WRF mesoscale model, allowing for both climatological estimates of icing and short term icing forecasts. The current model was able to detect periods of icing reasonably well at the warmer site. However at the cold climate site, the model was not able to remove ice quickly enough leading to large ice accumulations, which have not been seen in observations. In addition to the model evaluation we were able to investigate the potential occurrence of ice induced power loss at two wind parks in Europe using observed data. We found that the potential loss during an icing event is large even when the turbine is not shut down for its protection. We also found that there is a a large spread across the various turbines within a wind park, in the amount of icing. This is currently not taken into account by our model. Evaluating and adding these small scale differences to the model will be undertaken as future work.

1 Introduction

The occurrence of icing on wind turbines has been identified as an important issue when siting turbines in cold climates, due to the potential for production loss, structural fatigue, and health and safety issues. The ability to forecast turbine icing could help minimize these risks by helping to identify sites which are prone to excessive icing before they are constructed. Additionally the inclusion of icing in short term power production estimates is expected to improve those estimates, and make them more reliable in cold climate locations.

Currently there are two different prime areas of research surrounding icing on wind turbines. The first approach, utilized mostly by researchers looking to understand the fundamentals of ice growth on turbines, relies on advanced computation fluid dynamics models (CFD) to represent the airfoil in two or three dimensions and physically model the ice growth under steady state conditions. This approach is very computationally expensive, and currently only available for steady state problems. The second approach is a forecasting approach in which a mesoscale model is used to provide the required input parameters occurring at a given location into a simplified icing model which determines how much ice will exist. The icing model most commonly used for this approach is the Makkonen model [8]. The Makkonen model is the model used in the ISO standard for icing on wind turbines, and was developed to estimate the amount of ice growth on a freely rotating cylinder. The current forecasting models, have demonstrated accuracy when representing icing on a cylinder, but have been unable to capture the differences between the icing which occurs on a cylinder and that which occurs on a turbine [2, 3]. This study uses a similar approach to the previous studies, but has replaced the Makkonen model with an analytical solution to the 3

*Corresponding Author Email: neda@dtu.dk; Dir: +45 4677 5067

phase Stefan problem developed by Brakel et al [1]. In addition to the amount of ice growth, the Brakel model is able to estimate the type of ice which is expected to grow (rime or glaze) and has additional features which will allow it to incorporate deicing technologies in the future.

The two wind farms selected for this study are located in very different climates and topographic regions. Site A is located in a mountainous region of the Iberian peninsula, while Site B is located in a relatively flat, forested region of Sweden. Both sites are known to have experienced icing related issues in the past, and the periods of study were focused around times when the probability of icing events was large. Through this study we were able to find that the current model is able to detect icing periods fairly well at site A, while not able to detect the end of icing periods at all for site B. We also found, in examining the data of the two wind farms, that there is a wide spread in the impact of icing depending on the turbine being studied.

2 Methods

2.1 Observations

The turbine and meteorological observations provided for the two sites differed greatly, but both sites provided enough information that we feel we were able to capture the instances of icing at the sites. The differences in data availability did require different filtering techniques for the two sites. Also at the request of the data providers, all production data was normalized.

At both sites an estimated power was calculated using the nacelle wind speeds. To calculate this estimated power we utilized estimated power curves provided by the WAsP model. These estimated power values are compared against the actual data in section 3.1.

Site A provided us with mast based temperature data, nacelle wind speeds, power production, turbine RPM data, and the output from the SCADA system for the winter of 2010-2011. The SCADA output was particularly beneficial as it included a flag for icing based on internal settings of the turbine. This provided a robust dataset with which we could evaluate our model. All data for site A was filtered by removing wind speeds above and below the cutoff levels. In examining this data we chose to focus on a period of 10 days during the end of November, early December where there was a long period of icing detected.

Site B provided nacelle wind speeds, temperature, and power production for the entire month of January 2011. Because this site did not have a flag to indicate icing, the availible data was utilized to create one. Icing was determined to exist, when the nacelle temperature was below 0°C and the actual power was less than 80% of the estimated power, the period was identified as having ice. In addition to not having an icing flag, we were not provided with any flags from the turbine at this site, so we were unclear as to what state the turbine was in when there was no power being generated. We therefore chose to filter all times with no power production from site B, in addition to applying the cutoff filters applied at site A.

2.2 WRF Modeling

To provide meteorological input into the ice model the WRF mesoscale model version 3.3 [10] was used. At both locations we tested three different of microphysical schemes (SUNY-Lin [7], Thompson [11], WSM5 [4]) each paired with three different planetary boundary layer (PBL) schemes (MYJ [6], MYNN2 [9], YSU [5]). The microphysical schemes control the development of clouds and precipitation in the model during non-convective periods. While the PBL schemes calculate the mixing and flux terms of momentum, heat, and moisture in the mesoscale model. We felt it was important to test different schemes both to determine the robustness of our results, and to evaluate which schemes best capture the parameters required for icing estimation. All model runs used the NCEP FNL (Final) operational global analysis dataset for initial and boundary conditions, and employed grid based nudging on the outermost domain. Due to the grid based nudging, the outermost nest was not used for any analysis.

At site A, we focused on a 10 day period in late November to early December 2010. WRF was run for each of the 10 days, with a 12 hour spin-up period, followed by a 48 hour forecast period. All results presented here are from the second day forecast or hours 25-48, however the results

did not change much if the first day forecast was used instead. WRF was run with three nested domains, the first nest had a 24 km resolution, with the other two domains at 8 km and 2.667 km resolution.

At Site B, the WRF model was run to match the provided observational period, January 2011. Over this period, WRF was run was run in 10 day chunks with a 24 hour spin-up period. Due to the longer period, WRF was run with only two nests for site B, the outermost nest was run at 30 km resolution and the inner nest at 10 km resolution.

2.3 Ice Model

The ice model was developed based on the Brakel model [1] with a collision efficiency taken from the Makkonen model [8], and the inclusion of a simplified ice ablation algorithm. The Brakel ice growth model is an asymptotic model which calculates the temperature at which ice forms, whether that ice is rime ice or glaze ice, and finally the amount of ice which will be created under given conditions. We input varying cloud mass flux, temperature, wind speed, Lewis number, density and pressure values. Additionally constants were provided for the blade thermal conductivity (1.0 $\mathrm{W/m\,K}$), convective heat transfer coefficient between air and the substrate (2000 $\mathrm{W/m^2\,K}$), and the blade thickness (1 cm).

Most parameters were either taken directly from the WRF model or easily calculated from those results, these included the ambient temperature, pressure, density, and humidity at the approximate hub height of the turbine. Two terms which required additional processing were the cloud mass flux, and the wind speed. To calculate the cloud mass flux striking the turbine blade, we first calculated the total cloud mass flux from the WRF output. Then the Makkonen collision efficiency equation (α_1) was utilized to determine the amount of the total cloud mass would reach the blade. For this equation, we assumed a constand median volumetric diameter of 5 micrometers, and a 0.144 diameter cylinder to represent the leading edge of the turbine blade. To calculate the wind speed used for the Brakel model we had to relate the WRF ambient wind speed to the rotational speed of the turbine, and then relate that rotational speed to a linear speed at a given point on the blade. The rotational speed was derived from the observed data at site A, and the linear speed was calculated at 75% of the blade length.

The final piece of the ice model is the ice removal algorithm. The current model only accounts for ice removal through melting and sublimation, neglecting the shedding term, which potentially has the largest impact, but is the most challenging to model. Both melting and sublimation are based on the energy balance of the environment during times of non-ice growth. The radiative fluxes of interest are the sensible heat flux, calculated based on the difference between the air and ice temperature (melting only), the latent heat flux, calculated based on the difference between the air and ice vapor pressures, and the short-wave and long-wave radiation balance. These three fluxes are combined to provide the energy required to either melt or sublimate the ice depending on the atmospheric temperature. When the temperature is above freezing, melting occurs, otherwise sublimation occurs. Both the sensible and latent heat fluxes are found based on a temperature difference and the convective heat transfer coefficient.

In addition to the physical ice model, we utilized a threshold method for determining icing periods on turbines. This method used the raw temperature and cloud mixing ratio output of the WRF model to determine ongoing icing. The thresholds were set at 0°C and .05 g/kg respectively. Results from both models are compared.

3 Results

3.1 Observations

Having detailed observations at multiple turbines within two distinct wind parks allowed us to investigate the impact of icing on individual turbines in addition to the park as a whole. Before we could evaluate our icing model, we needed to determine the impact of icing on these two sites. To do that we started by investigating the deviation of the actual power output from the estimated power curve under different conditions. Figure 1 shows the actual and estimated power curves

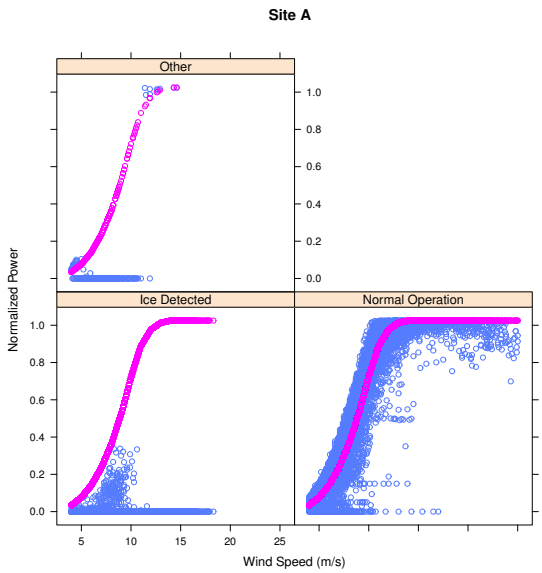

Figure 1: Estimated (pink) and actual (blue) power curves for Site A. Grouping areas indicate turbine status.

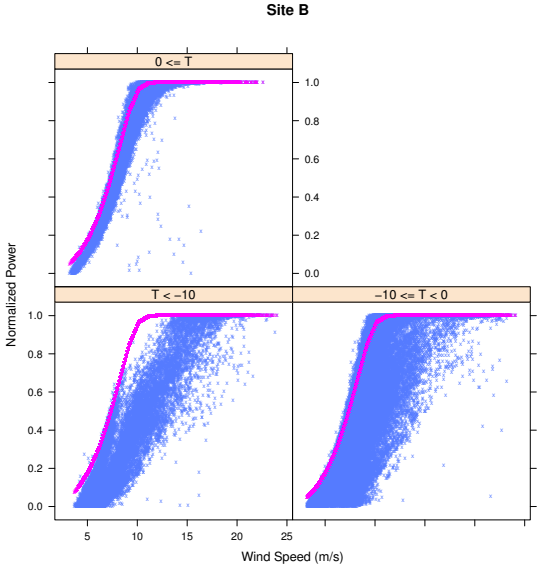

Figure 2: Estimated (pink) and actual (blue) power curves for Site B. Grouping is based on observed nacelle temperatures in °C.

for site A, grouped by turbine status. From this it can be seen that the majority of the time when the turbine is detecting icing there is no power being produced. This indicates that the turbine has been shut down due to the icing flag. The shut down has lead to a large amount of non-obtained potential power. We calculated that during the periods flagged as icing, the turbines captured less than 1% of the available energy. Additionally we found large variations across the almost 20 turbines as to the amount of time the turbine was in the icing state, between 3% and 47% of the 10 day period.

At site B, the icing status flag was not availible, so we compared the power output based on different temperature bins. Figure 2 shows that for temperatures above 0°C the site shows good agreement with the estimated power curve. However, for temperatures below 0°C there is much larger scatter, and at temperatures below -10°C the turbine is unable to reach the knee of the power curve. Because we do not have detailed status information from this site, we cannot be certain that this deviation from the power curve is strictly due to icing, but due to the good agreement at temperatures above freezing, we feel it is a reasonable assumption to make.

As at site A, site B showed fairly large discrepancies in the power lost at colder temperatures at the various turbines. Site B had almost 50 turbines, and it was found after removing periods of 0 production, due to the uncertainty of the cause of the shut down, that when the temperature was below 0, and the turbine was under performing, that the power loss varied from 7-20% of the potential power.

When looking at the wind farm in total, we found that the lost power varied greatly depending on the temperature range we were investigating. When the temperature was below -10°C only 64% of the estimated available energy was captured, while at temperatures between -10°C and 0°C, 93% was captured, and at temperatures above freezing 101% of the estimated available energy was captured. The 101% value shows one of the limitations of using the generic power curve for estimating power loss due to icing, however these results still appear to be robust.

3.2 Ice Model Forecasts

To evaluate the performance of the ice model we focused on three results, the models icing period compared with the observed icing period, the active icing period compared with the observed icing period, and the ice height over time of the icing model.

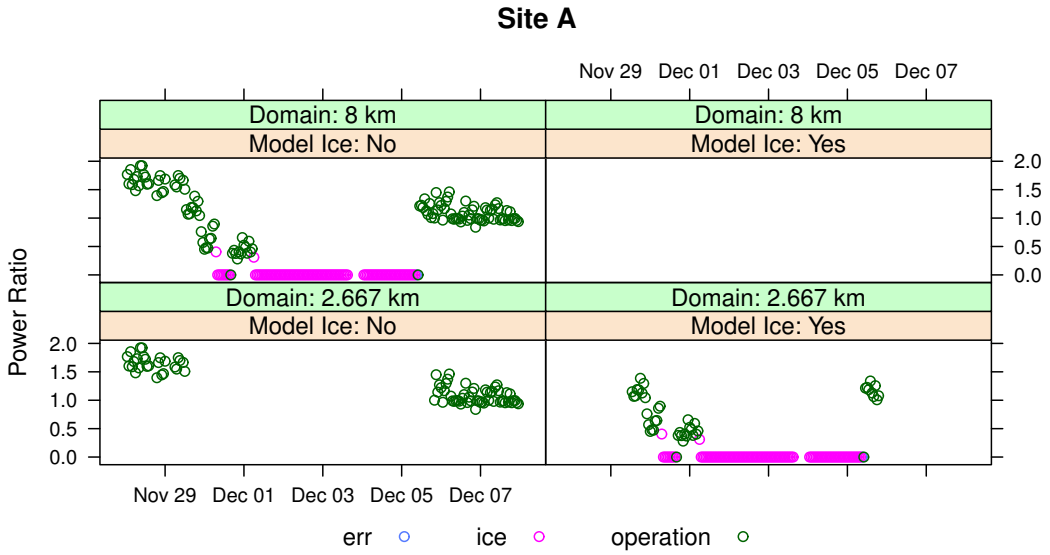

Figure 3: Power ratio (actual power / estimated power) at a selected turbine, compared with model icing. The Thompson microphysics and MYNN2 PBL schemes were used for this plot. The top figures are from the 8 km model simulation, and the bottom figures are from the 2.667 km simulation. The left figures are when the model does not predict ice, while the right figures are when the model predicts ice. Finally the colors are based upon the turbine status flag.

3.2.1 Site A

For site A, we first examined the model result compared with one of the turbines at the site (Fig. 3). This turbine was one of the most affected on the site, experiencing icing more than 40% of the period. We found that the 8 km mesoscale domain was unable to simulate the conditions which lead to the icing event. However, the 2.667 km domain was able to pick out the period when the icing event occurred, with reasonable accuracy. The icing model was slightly early in detecting the icing, which could have to do with a required amount of build up on the blades before the icing will trigger an alarm. Also the model appears to be too slow in removing the ice from the blades as the period of normal operation in the middle of the period is missed, in addition to the model missing the timing of the end of the event.

We next examined the results of the physical model compared to the threshold method. Figure 4 shows the periods of time four different methods predict icing to be occurring. The ”observed” dataset is based on the turbine status flag. The ”accumulated” dataset is based on the full physical ice model. The ”active” dataset is based on when the physical ice model detects ice actively growing on the blade, and the ”thresh” dataset is the periods where the threshold method determined there would be ice occurring. From this it appears the threshold method identifies more periods than the active icing method, but both miss the majority of the observed icing period due to the lack of ice persistence in those methods. The accumulated method best matches the observed dataset, although it too has some limitations as shown in figure 3.

Next we looked at the ice height forecast from the icing model, using the results from the 9 different WRF simulations as input. This result was not able to be compared with observations, however from images of other sites, it seems the maximum thickness on a blade is never over 5 cm. The icing model kept within this range at this site for all 9 simulations. It was shown that the SUNY-Lin scheme consistently forecast the lowest amount of ice growth, while the Thompson scheme consistently forecast the most. The WSM5 scheme was shown to be the most sensitive to which PBL scheme it was coupled. One thing we noted from this study was that the ice growth can be very rapid, up to 5 mm in an hour, while the ice removal is much slower. This is likely due to the model not including shedding which is the most rapid form of ice removal.

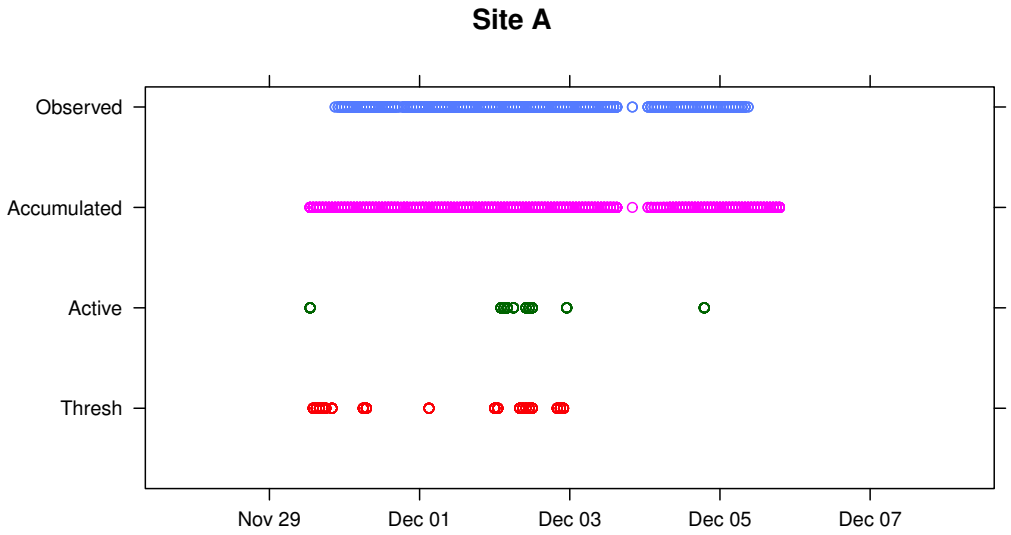

Figure 4: Period of time where icing was observed or predicted to occur. Same turbine and WRF physics as Figure 3, and the simulated meteorological conditions from the 2.667 km domain were used.

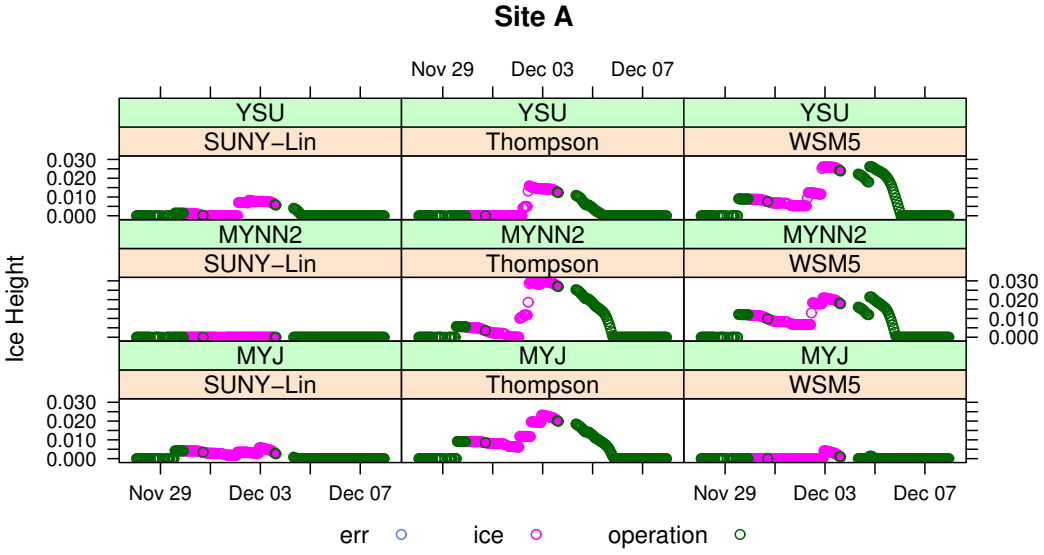

Figure 5: Ice height (m) over time from each of the 9 mesoscale physics options at site A. Colors are based on the turbine status flag. The 2.667 km domain was used.

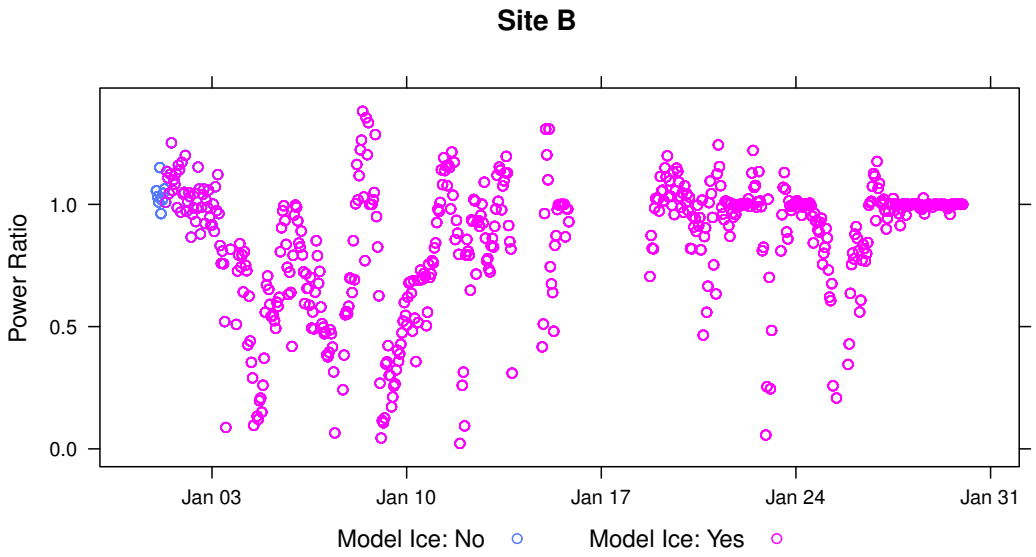

Figure 6: Power ratio (actual power / estimated power) at a selected turbine, compared with model icing. The Thompson microphysics and MYNN2 PBL schemes were used for this plot. Finally the colors are based upon the model icing flag.

3.2.2 Site B

Unlike at site A, at site B we see that once ice occurs in the model, it is never removed. This is most likely not what happened in the actual case as indicated by the large number of points near 1.0 power ratio during the last 5 days of the month (Fig. 6). We have examined this period and found the temperature to be above 0°C during this period, so it is doubtful that there would have still been ice on the turbine during this period. As with site A, we attribute this to the lack of a shedding removal mechanism.

When comparing the active icing to the threshold icing, we see opposite results from those at site A (fig. 7), with the active icing dataset showing more icing than the threshold method. This is most likely due to the different limiting factors at the two sites. At site B, the limiting factor was mostly the water availability, since the temperature was consistently far below the freezing point. The reduced amount of ice periods via the threshold method suggests that for cold climate sites, the threshold may be too high. At site A the limiting factor to icing is the temperature. Because the temperature is closer to the freezing point, there are times where there is enough moisture for the threshold method to detect ice, but the Brakel model predicts that the incoming mass flux is too great and would heat the surface above freezing, not allowing ice to form.

When examining the height graph of site B, we see some of the same features as at site A (fig. 8). The model shows many periods of rapid ice growth, but only very small ice removal. It is this very small ice removal which appears to be driving the model to ever increasing amounts of ice during the period. Similar to site A, the SUNY-Lin microphysical scheme shows little ice growth compared to the other two schemes. In the Thompson and WSM5 schemes the ice growth is very large, reaching over 1 m in length in all 6 model runs with those microphysics. Additionally we are able to see that the model mostly predicted rime ice growth at this site, again suggesting very cold temperatures when icing was occuring.

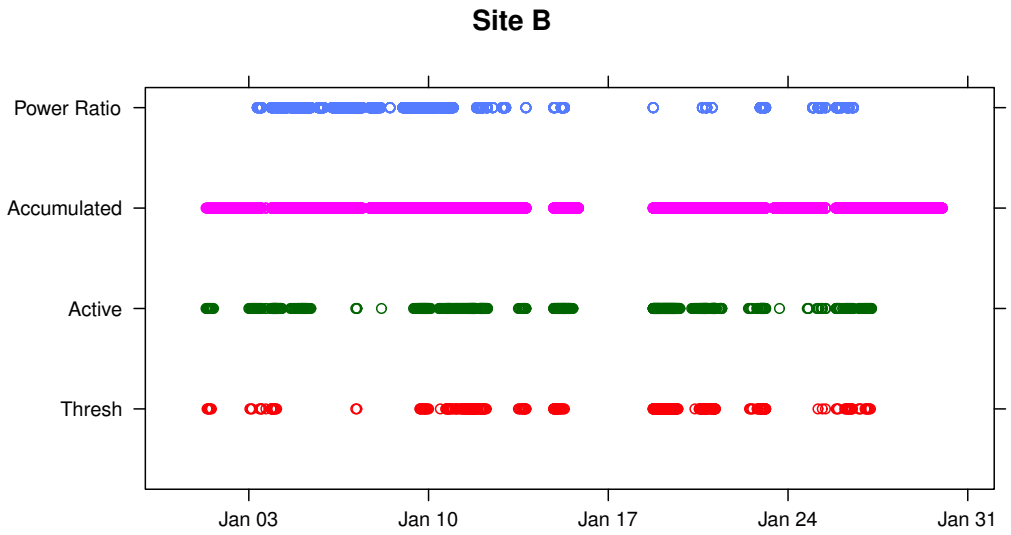

Figure 7: Period of time where icing was observed or predicted to occur. Same turbine and WRF physics as Figure 6.

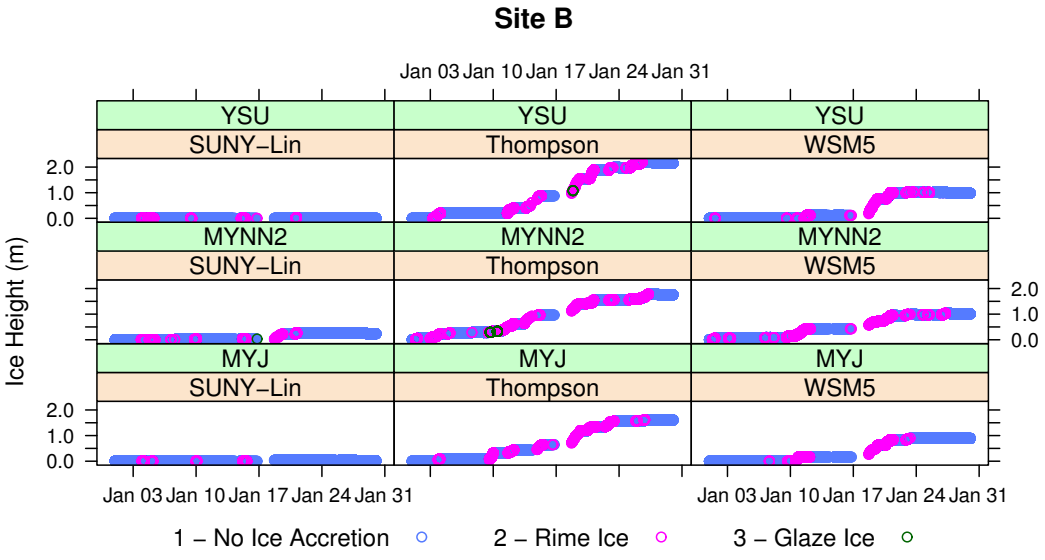

Figure 8: Ice height (m) over time from each of the 9 mesoscale physics options at site A. Colors are based on the ice type from the model. The 10 km domain was used.

4 Conclusion

In this study we showed that icing can lead to major losses, even at sites with moderate climates such as the Iberian Peninsula. We also illustrated that our icing model can do a reasonable job of representing ice accretion on a turbine in moderate climates. However we found that in cold climates the current model grows ice much faster than it is removed leading to very large ice amounts, and the inability to estimate the end of icing events. With this knowledge we hope to further advance our icing model to better represent sites in cold climates.

5 Future Work

The next steps for this project involve finding improvements to the ice removal algorithms, first by adding a random ice shedding term, and then by looking to improve our calculation of the sensible and latent heat terms. After adding these new terms, we will look to evaluate the model over additional locations and for longer periods of time. Once we feel we are able to represent the periods of icing with our model, we will look to relate the ice height parameter with production loss.

References

[1] T.W. Brakel, J.P.F. Charpin, and Tim G. Myers. One-dimensional ice growth due to incoming supercooled droplets impacting on a thin conducting substrate. *International Journal of Heat and Mass Transfer*, 50(9-10):1694–1705, May 2007.

[2] Øyvind Byrkjedal. Mapping of icing in Sweden On the influence from icing on wind energy production. In *Winterwind*, Skellefteå, Sweden, 2012.

[3] Pau Casso, Gil Lizcano, Pep Moreno, and Josep Calbo. Evaluation of WRF mesoscale model for icing events characterization, some insights on model performance, limits and capabilities. In *Winterwind*, Skellefteå, Sweden, 2012.

[4] Song-You Hong, Jimy Dudhia, and Shu-Hua Chen. A Revised Approach to Ice Microphysical Processes for the Bulk Parameterization of Clouds and Precipitation. *Monthly Weather Review*, 132(1):103–120, January 2004.

[5] Song-You Hong, Yign Noh, and Jimy Dudhia. A New Vertical Diffusion Package with an Explicit Treatment of Entrainment Processes. *Monthly Weather Review*, 134(9):2318–2341, September 2006.

[6] Zaviša I. Janjić. The Step-Mountain Eta Coordinate Model: Further Developments of the Convection, Viscous Sublayer, and Turbulence Closure Schemes. July 2009.

[7] Yanluan Lin and Brian a. Colle. A New Bulk Microphysical Scheme That Includes Riming Intensity and Temperature-Dependent Ice Characteristics. *Monthly Weather Review*, 139(3):1013–1035, March 2011.

[8] Lasse Makkonen. Models for the growth of rime, glaze, icicles and wet snow on structures. *Philosophical Transactions of the Royal Society of London. Series A: Mathematical, Physical and Engineering Sciences*, 358(1776):2913–2939, 2000.

[9] Mikio Nakanishi and Hiroshi Niino. An Improved MellorYamada Level-3 Model: Its Numerical Stability and Application to a Regional Prediction of Advection Fog. *Boundary-Layer Meteorology*, 119(2):397–407, March 2006.

[10] William C. Skamarock, Joseph B. Klemp, Jimy Dudhia, David O. Gill, Dale M. Barker, Michael G. Duda, Xiang-Yu Huang, Wei Wang, and Jordan G. Powers. A Description of the Advanced Research WRF Version 3, 2008.

[11] Gregory Thompson, Paul R. Field, Roy M. Rasmussen, and William D. Hall. Explicit Forecasts of Winter Precipitation Using an Improved Bulk Microphysics Scheme. Part II: Implementation of a New Snow Parameterization. *Monthly Weather Review*, 136(12):5095–5115, December 2008.

Financial support for this project is provided by the Top-Level Research Initiative (TFI) project, Improved forecast of wind, waves and icing (IceWind) and Vestas.

*Corresponding Author Email: neda@dtu.dk; Dir: +45 4677 5067